



## Tunability and Noise Dependence in Differentiation Dynamics

Gürol M. Süel, *et al.*  
*Science* **315**, 1716 (2007);  
DOI: 10.1126/science.1137455

**The following resources related to this article are available online at [www.sciencemag.org](http://www.sciencemag.org) (this information is current as of March 22, 2007):**

**Updated information and services**, including high-resolution figures, can be found in the online version of this article at:

<http://www.sciencemag.org/cgi/content/full/315/5819/1716>

**Supporting Online Material** can be found at:

<http://www.sciencemag.org/cgi/content/full/315/5819/1716/DC1>

This article **cites 20 articles**, 7 of which can be accessed for free:

<http://www.sciencemag.org/cgi/content/full/315/5819/1716#otherarticles>

This article appears in the following **subject collections**:

Cell Biology

[http://www.sciencemag.org/cgi/collection/cell\\_bio](http://www.sciencemag.org/cgi/collection/cell_bio)

Information about obtaining **reprints** of this article or about obtaining **permission to reproduce this article** in whole or in part can be found at:

<http://www.sciencemag.org/about/permissions.dtl>

10. K. L. Pierce, R. T. Premont, R. J. Lefkowitz, *Nat. Rev. Mol. Cell Biol.* **3**, 639 (2002).
11. A. M. Spiegel, L. S. Weinstein, *Annu. Rev. Med.* **55**, 27 (2004).
12. H. Ma, M. Yanofsky, E. M. Meyerowitz, *Proc. Natl. Acad. Sci. U.S.A.* **87**, 3821 (1990).
13. H. Ma, *Plant Mol. Biol.* **26**, 1611 (1994).
14. M. G. Mason, J. Botella, *Proc. Natl. Acad. Sci. U.S.A.* **97**, 14784 (2000).
15. M. G. Mason, J. R. Botella, *Biochim. Biophys. Acta* **1520**, 147 (2001).
16. A. M. Jones, S. A. Assmann, *EMBO Rep.* **5**, 572 (2004).
17. S. Plakidou-Dymock, D. Dymock, R. Hooley, *Curr. Biol.* **8**, 315 (1998).
18. G. Colucci, F. Apone, N. Alyshermi, D. Chalmers, M. J. Chrispeels, *Proc. Natl. Acad. Sci. U.S.A.* **99**, 4736 (2002).
19. S. Pandey, S. M. Assmann, *Plant Cell* **16**, 1616 (2004).
20. S. M. Assmann, *Science* **310**, 71 (2005).
21. P. Obrdlík et al., *Proc. Natl. Acad. Sci. U.S.A.* **101**, 12242 (2004).
22. X.-Q. Wang, H. Ullah, A. M. Jones, S. M. Assmann, *Science* **292**, 2070 (2001).
23. J. M. Ward, Z. M. Pei, J. I. Schroeder, *Plant Cell* **7**, 833 (1995).
24. S. R. Sprang, *Annu. Rev. Biochem.* **66**, 639 (1997).
25. S. Pandey, J. G. Chen, A. M. Jones, S. M. Assmann, *Plant Physiol.* **141**, 243 (2006).
26. We thank D. Y. Sun for his support; X. W. Deng and J. M. Zhou for their comments and discussion; W. Frommer and P. Obrdlík for making the split-ubiYFP system available; J. Kuala for making the split-YFP system available; J. Chai for his technical assistance and advice for the protein purification; and D. Zhang, Y. Shen, and

F. Razem for their suggestions on the ABA binding assay. This work was supported by the Ministry of Science and Technology of China (to L.M., 2003AA210120), National Science Foundation of China for Outstanding Young Scientists (to L.M., 30025024) and the Chinese National Key Basic Research Project (to W.W., 2006CB100100).

### Supporting Online Material

www.sciencemag.org/cgi/content/full/1135882/DC1  
Materials and Methods  
Figs. S1 to S11  
References

3 October 2006; accepted 24 January 2007

Published online 8 March 2007;

10.1126/science.1135882

Include this information when citing this paper.

# Tunability and Noise Dependence in Differentiation Dynamics

Gürol M. Süel,<sup>1</sup> Rajan P. Kulkarni,<sup>2</sup> Jonathan Dworkin,<sup>3</sup> Jordi Garcia-Ojalvo,<sup>4</sup> Michael B. Elowitz<sup>2\*</sup>

The dynamic process of differentiation depends on the architecture, quantitative parameters, and noise of underlying genetic circuits. However, it remains unclear how these elements combine to control cellular behavior. We analyzed the probabilistic and transient differentiation of *Bacillus subtilis* cells into the state of competence. A few key parameters independently tuned the frequency of initiation and the duration of competence episodes and allowed the circuit to access different dynamic regimes, including oscillation. Altering circuit architecture showed that the duration of competence events can be made more precise. We used an experimental method to reduce global cellular noise and showed that noise levels are correlated with frequency of differentiation events. Together, the data reveal a noise-dependent circuit that is remarkably resilient and tunable in terms of its dynamic behavior.

Three aspects of genetic circuits control dynamic cellular behaviors: the circuit architecture or pattern of regulatory interactions among genetic elements; quantitative parameter values, such as promoter strengths; and stochastic fluctuations, or “noise,” associated with the concentration of cellular components. A fundamental biological question is how these three aspects of genetic circuits combine to determine cellular behavior, its variability, and its potential to evolve (*1*).

Competence in *B. subtilis* is a stress response that allows cells to take up DNA from the environment (*2, 3*). Differentiation into competence is transient (Fig. 1A) (*4*). The genetic basis for this behavior is a circuit involving *comK* and *comS* (Fig. 1B). The transcription factor ComK is necessary and sufficient for differentiation into competence (*5, 6*). ComK positively autoregulates its

own expression but is degraded by the ClpP-ClpC-MecA protease complex (Fig. 1B) (*7–9*). ComS competitively inhibits this degradation and is repressed in competent cells, forming a negative feedback loop (*4, 10, 11*). The circuit operates as

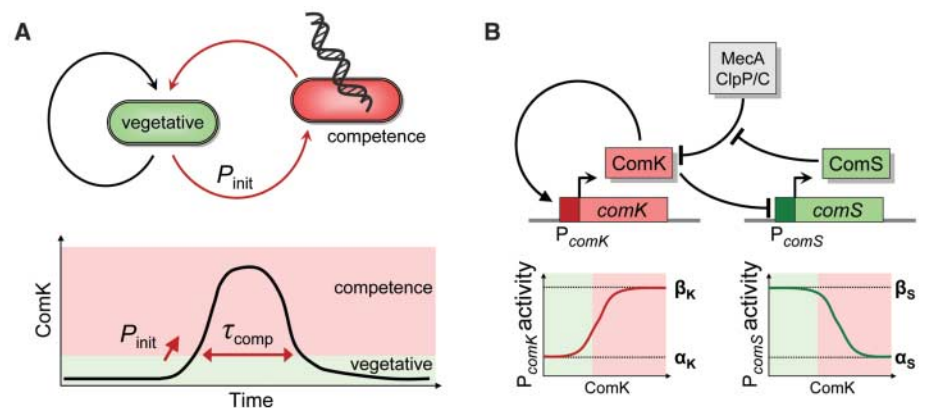


**Fig. 1.** Competence is a probabilistic and transient differentiation process regulated by a genetic circuit. **(A)** The rate of entering the competent state from the vegetative state is denoted by  $P_{init}$ . The amount of time spent in the competent state is denoted by  $\tau_{comp}$ . The ComK transcription factor concentration is high (pink region) when cells are competent and low (green region) when they are growing vegetatively. **(B)** Map of the core competence circuitry. Key features include positive transcriptional autoregulation of ComK and a negative feedback loop in which ComK inhibits (possibly indirectly) expression of ComS, which in turn interferes with degradation of ComK. The graphs below the  $P_{comK}$  and  $P_{comS}$  promoters define parameters used in the text: Expression rates change from  $\alpha_K$  to  $\beta_K$  and  $\beta_S$  to  $\alpha_S$  respectively, as ComK concentration increases during competence.

<sup>1</sup>Green Center Division for Systems Biology and Department of Pharmacology, University of Texas Southwestern Medical Center, Dallas, TX 75390, USA. <sup>2</sup>Division of Biology and Department of Applied Physics, California Institute of Technology, Pasadena, CA 91125, USA. <sup>3</sup>Department of Microbiology, College of Physicians and Surgeons, Columbia University, New York, NY 10032, USA. <sup>4</sup>Departament de Física i Enginyeria Nuclear, Universitat Politècnica de Catalunya, Colom 11, E-08222 Terrassa, Spain.

\*To whom correspondence should be addressed. E-mail: melowitz@caltech.edu

strains, respectively [see Supporting Online Material (SOM) text]. To systematically scan a range of values for  $\alpha_K$  and  $\alpha_S$ , we made time-lapse fluorescence movies of these strains on media containing different concentrations of the inducer isopropyl- $\beta$ -D-thiogalactopyranoside (IPTG) (Fig. 2, A and B).

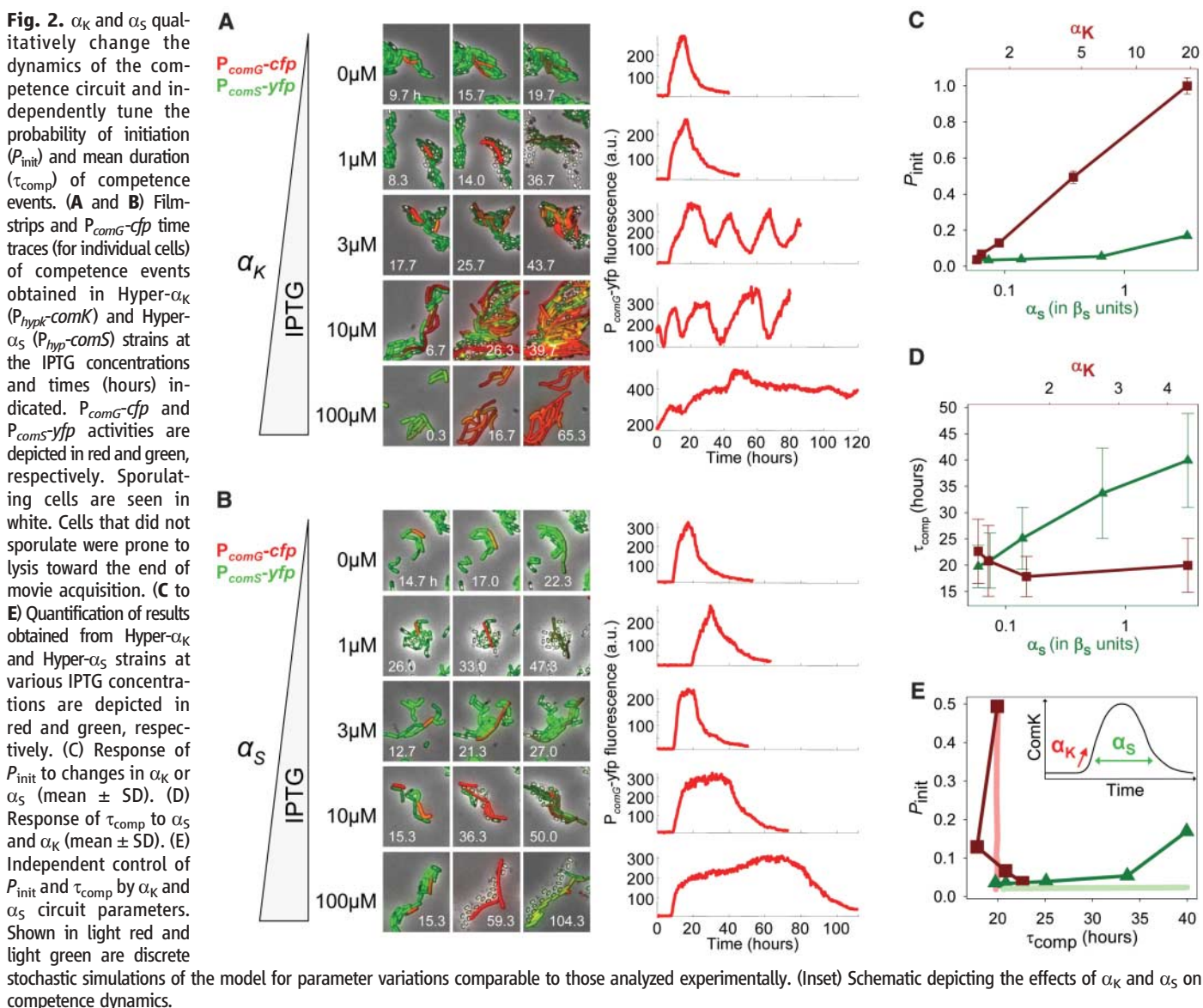
We investigated how  $\alpha_K$  and  $\alpha_S$  combine to regulate  $P_{init}$ . Without IPTG,  $P_{init}$  was  $\sim 3\%$  in the Hyper- $\alpha_K$  strain, unchanged from its wild-type value.  $P_{init}$  increased rapidly with basal *comK* expression (Fig. 2C). Increased expression of *comK* in the Hyper- $\alpha_K$  strain also showed a transition to an oscillatory regime, in which cells repeatedly went in and out of the competent state (Fig. 2A). At  $\alpha_K \sim 20$  times its wild-type value,  $\alpha_K^{wt}$ , all cells entered competence (Fig. 2, A and C). *ComS*, like *ComK*, is necessary for competence. However, expression of  $P_{hyp-comS}$  had a modest effect on initiation, increasing  $P_{init}$  to  $\sim 20\%$  (Fig. 2C). Thus,  $P_{init}$  was predominantly regulated by  $\alpha_K$  rather than  $\alpha_S$ .

We next considered the effects of the same perturbations on  $\tau_{comp}$ . Increasing  $\alpha_K$  up to  $\sim 4.5 \times \alpha_K^{wt}$  caused no increase in  $\tau_{comp}$  (Fig. 2D). On the other hand, in the Hyper- $\alpha_S$  strain,  $\tau_{comp}$  increased with increasing expression of  $P_{hyp-comS}$  (Fig. 2D). Thus,  $\tau_{comp}$  was predominantly regulated by  $\alpha_S$  rather than  $\alpha_K$ . Together, these results show that  $P_{init}$  and  $\tau_{comp}$  can be tuned independently by  $\alpha_K$  and  $\alpha_S$ , respectively (Fig. 2E).

To better understand the effect of *comS* expression on  $\tau_{comp}$ , we constructed a “6 $\times$ S” strain in which  $P_{comS-comS}$  was expressed from a low-copy number plasmid, effectively increasing the activated production rate,  $\beta_S$ , by a factor of 6 over its wild-type value,  $\beta_S^{wt}$ . Unlike  $P_{hyp-comS}$ , this construct retains the regulation found in the wild-type  $P_{comS}$  promoter, including its negligible basal expression rate,  $\alpha_S^{wt}$ . Despite this increase in  $\beta_S$ , excitable behavior was maintained, as  $53 \pm 5\%$  ( $n = 79/151$ ) of competent cells successfully exited the competent state, compared with  $61\% \pm 7\%$  ( $n = 83/136$ ) of wild-type cells. By contrast,

increasing  $\alpha_S$  to  $\sim 3 \times \beta_S^{wt}$  in the Hyper- $\alpha_S$  strain prevented the majority of competent cells from exiting [ $21.3 \pm 5\%$  ( $n = 26/122$ ) of competent cells exited (table S4)]. The repressibility of the natural  $P_{comS}$  promoter is thus critical for maintaining excitability (4). These results show that excitability can be reliably maintained over a broad range of  $\beta_S$  values.

To better understand independent tuning of  $P_{init}$  and  $\tau_{comp}$ , as well as reliable maintenance of excitability, we developed a model of the core interactions in the competence regulation circuitry (Fig. 1B and SOM text). We used stochastic simulations to account for intrinsic noise of biochemical reactions (14). We also analyzed the corresponding continuous model to determine parameter dependence and to identify a biologically reasonable parameter regime in which the discrete model produced results consistent with experiments. We required the continuous model to remain in the excitable regime as the  $\beta_S$  value was varied by a factor of 6



and we required its stochastic counterpart to generate the observed independent tunability of  $P_{init}$  and  $\tau_{comp}$ . We identified a parameter set that accounts for both maintenance of excitability at high  $\beta_S$  and independent tunability by  $\alpha_S$  and  $\alpha_K$ . Analysis of the model is described in detail in the SOM text (15).

Within the model, increasing  $\alpha_K$  increased the probability that vegetative cells reach the minimum concentration of ComK necessary to initiate competence, explaining the strong effect of  $\alpha_K$  on  $P_{init}$  (Fig. S5). Increasing  $\alpha_S$ , on the other hand, did not raise  $P_{init}$  arbitrarily high because initiation of competence is limited by fluctuations in ComK expression (Fig. 2E and fig. S6).

In the model, we also analyzed  $\tau_{comp}$ . Exit from competence requires ComS to be degraded. When the basal production rate of ComK is less than its activated production rate ( $\alpha_K < \beta_K$ ), ComS degradation, and thus  $\tau_{comp}$ , is unaffected. On the other hand, as  $\alpha_S$  is increased from zero, production of ComS offsets its degradation, prolonging competence duration.

Consistent with experimental results, in the model increasing  $\alpha_K$  switches the system from excitable to oscillatory dynamics, further distinguishing  $\alpha_K$  from  $\alpha_S$  (fig. S3). Increasing  $\alpha_S$  takes the system directly from excitability to a bistable regime in which  $P_{init} < 1$ , but, once initiated, most cells remain trapped in the competent state. This behavior was also observed in experiments where no oscillatory behavior was seen at intermediate  $\alpha_S$  values (Fig. 2B).

As in the experiments, cells in the model can become stuck in competence. When the basal production rate of ComK exceeds its activated production rate ( $\alpha_K > \beta_K$ ), ComK levels cannot be reduced in competence, and cells become trapped in the competent state. A similar effect occurs at high  $\alpha_S$  values, because a new stable state arises at competence-maintaining concentrations of ComK (Fig. S7). However, in this case, exit of competence remained possible as a result of noise, which destabilizes the newly formed competent state (see Section S1.4 of SOM text). This is consistent with experimental observations showing that, even at the highest induction levels in the Hyper- $\alpha_S$  strain, ~20% of cells successfully exited competence.

To explore the effects of perturbing the circuit architecture, we reengineered the competence circuit using Rok, a protein that binds to  $P_{comK}$  and represses its expression (16). We inserted a copy of *rok* under the control of  $P_{comG}$ , creating an additional negative feedback loop onto *comK* (Fig. 3A). In this “CompRok” strain, as expected,  $P_{init}$  remained unchanged from its wild-type values (~3%). The mean value of  $\tau_{comp}$ , on the other hand, was reduced, as was its cell-cell variability. In CompRok,  $\tau_{comp} = 13.9 \pm 3.4$  hours (mean  $\pm$  SD,  $n = 30$ ), compared with  $\tau_{comp} = 20.2 \pm 9.9$  hours (mean  $\pm$  SD,  $n = 31$ ) in wild type (Fig. 3B). This reduction in cell-cell variability showed that the precision of  $\tau_{comp}$  can be improved over its wild-type value. In the

model (Fig. 3B, insets), this result can be explained as follows: Exit from competence occurs when the absolute number of ComS molecules is

very low and the relative size of stochastic fluctuations therefore increases. These effects increase the variability in  $\tau_{comp}$ . In the CompRok strain,

**Fig. 3.** Architectural change to the MeKS circuit reduces variability of competence durations ( $\tau_{comp}$ ). (A) Competence circuit was rewired to introduce an additional transcriptional negative feedback loop onto *comK*, generating the CompRok strain. (B) Fluorescence time traces, normalized by their maximum value, from  $P_{comG}$ -*cfp* in the CompRok strain or the wild type. Traces have been aligned with respect to time of initiation of  $P_{comG}$  expression. For each panel, corresponding discrete stochastic simulations of CompRok and wild-type competence circuits are shown as insets.

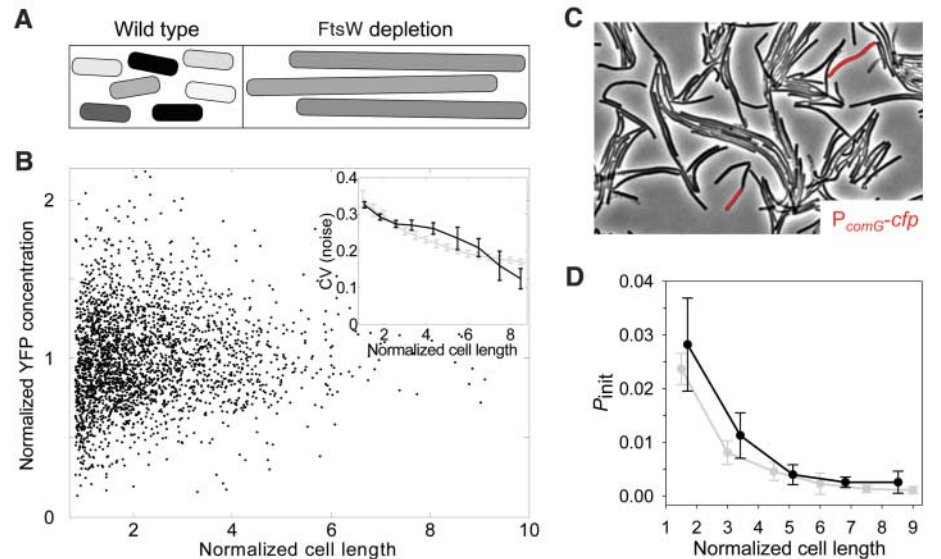
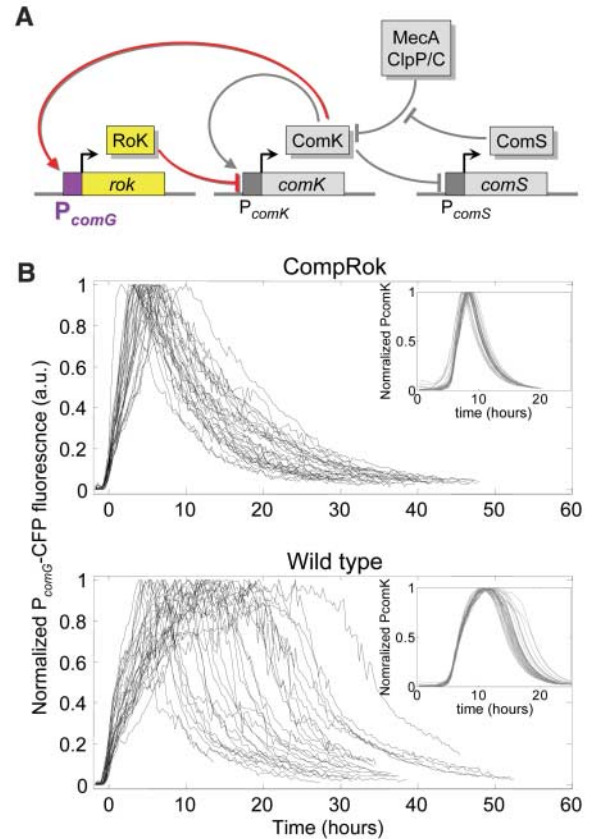


**Fig. 4.** Noise in gene expression and probability of competence initiation ( $P_{init}$ ) decreases with increasing cell length. (A) Cell-cell variation in gene expression (shades of gray) is expected to decrease in elongated conditional *ftsW* mutant cells compared with wild-type cells. (B) Noise decreases with increasing cell length: Dots represent  $P_{hyp}$ -*yfp* expression (normalized by mean) and length of individual conditional *ftsW* mutant (Fili-H) cells induced with 5  $\mu$ M IPTG. (Inset) Coefficient of variation (CV) of  $P_{hyp}$ -*yfp* expression as a function of cell length (black) compared with discrete stochastic model prediction (gray). (C) Overlay of phase contrast and  $P_{comG}$ -*cfp* fluorescence (red) snapshots of Fili-SOG cells with increased cell length. (D) Experimentally determined  $P_{init}$  (black line) drops with increasing cell length consistent with discrete stochastic simulations (gray line). Error bars in (C) and (D) denote one SD. (See S3.4 SOM text for details on calculation of  $P_{init}$ .)

however, the additional negative feedback allows exit from competence to occur at higher ComS and Rok concentrations, reducing the sensitivity of  $\tau_{\text{comp}}$  to stochastic fluctuations (fig. S10).

It is not known whether competence initiation is controlled by noise, as in the model. To test the impact of noise on competence initiation, we set out to globally modulate the amount of noise in the cell. We used a *B. subtilis* strain in which the *ftsW* gene, which is necessary for septation, was replaced by an inducible copy. In the absence of inducer, septation was inhibited, resulting in elongated filamentous cells. Each filament was composed of multiple cell units, all sharing cytoplasm. Within a filament, diffusion is expected to effectively average cell contents, reducing noise in gene expression, without affecting mean concentrations of cellular components (Fig. 4A) (17). In some bacterial mutants that have elongated filamentous morphologies, cellular growth, nucleoid density, protein expression, and other physiological characteristics appear normal, even though cellular volume is greatly increased (fig. S12) (18–20). We integrated an inducible  $P_{\text{hyp}}::yfp$  construct and measured the effect of cell length on cell-cell fluctuations in yellow fluorescent protein (YFP) expression (Fig. 4B). We found that noise does indeed decrease with increasing length (Fig. 4B, inset). A simple model of transcription and translation (21–24) that incorporates the continuity of filamentous cell growth produced qualitatively similar results (Fig. 4B, inset, and SOM text). Thus, cell size can in this case be used to modulate gene expression noise.

How does noise affect the probability of initiation of competence? To answer this question, we induced filamentation in the conditional *ftsW* strain at the beginning of, or before, movie acquisition and quantified  $P_{\text{init}}$  as a function of cell length. We determined length distributions of cells at the moment they initiated competence, as detected by  $P_{\text{comG}}$  expression (Fig. 4C). As a comparison, we also measured length distributions for noncompetent cells at a similar distribution of times. We plotted the relative fraction of cells that initiated competence at a given length, compared with the total number of cells at that length. The results showed that  $P_{\text{init}}$  decreased as cells elongated (Fig. 4D and SOM text). A similar decrease in  $P_{\text{init}}$  was observed in corresponding simulations (Fig. 4D). To test if the reduction in  $P_{\text{init}}$  could be due to factors other than diminished noise, we examined two promoters,  $P_{\text{comS}}$  and  $P_{\text{spo0A}}$ , both strongly regulated under these conditions. Spo0A is a master regulator of sporulation, a competing starvation response, and high concentrations of Spo0A inhibit competence (3). Conversely,  $P_{\text{comS}}$  expression is necessary for competence. Mean expression of both  $P_{\text{comS}}$  and  $P_{\text{spo0A}}$  was unaffected by cell length (fig. S17). This supports the idea that gene expression levels are independent of cell length under these conditions and that  $P_{\text{init}}$  depends on noise.

Noise may play at least three different functional roles in competence. First, noise could be

responsible for the observed variability in duration. Second, noise may be necessary to maintain excitability over a wide parameter range, by inducing escape from states of high ComK concentration. Third, noise appears to have a pivotal role in competence initiation (Fig. 4D) and thus should be considered alongside genetic parameters and circuit architecture to comprehensively understand differentiation at the single-cell level.

Quantitative analysis of a genetic system beyond its normal operating regime, including gene expression strengths, circuit architecture, and noise levels, strongly constrains dynamical models. The competence regulation system maintains excitable behavior over a broad range of parameter values. Experimentally,  $\alpha_K$  and  $\alpha_S$  enable  $P_{\text{init}}$  and  $\tau_{\text{comp}}$  to be tuned independently, allowing the system, in theory, to adapt to independent selective pressures during evolution. The circuit can also access different dynamic regimes, such as oscillation and bistability, indicating its potential to evolve alternative qualitative behaviors.

#### References and Notes

- U. Alon, *An Introduction to Systems Biology: Design Principles of Biological Circuits*. Mathematical and Computational Biology Series, vol. 10 (Chapman & Hall/CRC, Boca Raton, FL, 2006).
- A. D. Dubnau, *Annu. Rev. Microbiol.* **53**, 217 (1999).
- D. D. Grossman, *Annu. Rev. Genet.* **29**, 477 (1995).
- G. M. Suel et al., *Nature* **440**, 545 (2006).
- R. M. Berka et al., *Mol. Microbiol.* **43**, 1331 (2002).
- D. van Sinderen et al., *Mol. Microbiol.* **15**, 455 (1995).
- H. Maamar, D. Dubnau, *Mol. Microbiol.* **56**, 615 (2005).
- W. K. Smits et al., *Mol. Microbiol.* **56**, 604 (2005).
- K. Turgay et al., *EMBO J.* **17**, 6730 (1998).
- J. Hahn, L. Kong, D. Dubnau, *J. Bacteriol.* **176**, 5753 (1994).
- M. Ogura et al., *Mol. Microbiol.* **32**, 799 (1999).
- C. Koch, *Biophysics of Computation* (Oxford Univ. Press, Oxford, 1999).
- D. Dubnau, R. Losick, *Mol. Microbiol.* **61**, 564 (2006).
- D. T. Gillespie, *J. Phys. Chem.* **81**, 2340 (1977).
- The gene circuit shown in Fig. 1B can be described, in a continuous approximation, by two coupled differential equations that govern the dynamical evolution of the

concentrations of ComK and ComS proteins, denoted  $K$  and  $S$ , respectively. The equation for  $K$  is  $\frac{dK}{dt} = \alpha_K + \frac{\beta_K K^n}{K^n + K^{n-1} + 1} - \frac{\beta_K K}{1 + K/I_K + S/I_S} - \lambda_K K$ , where  $\alpha_K$  and  $\beta_K$  parameterize the strength of constitutive and autoregulated ComK expression, respectively. The third term models degradation through competitive binding of ComK and ComS to MecA. The final term represents linear degradation of ComK. The equation for  $S$  is  $\frac{dS}{dt} = \alpha_S + \frac{\beta_S}{1 + K/I_K + S/I_S} - \lambda_S S$ . Here,  $\alpha_S$  and  $\beta_S$  measure the strength of constitutive and regulated *comS* expression, respectively. The third and fourth terms represent MecA-mediated and linear degradation, respectively. Other parameters are defined in the SOM text. We have also developed a discrete model of the circuit that incorporates intrinsic noise explicitly. The requirement of independent tunability of  $P_{\text{init}}$  and  $\tau_{\text{comp}}$  strongly constrains the allowed parameter values and thus the structure of the phase space. The modeling is described in detail in the SOM text.

- T. T. Hoa et al., *Mol. Microbiol.* **43**, 15 (2002).
- M. B. Elowitz et al., *J. Bacteriol.* **181**, 197 (1999).
- F. Ishino et al., *J. Bacteriol.* **171**, 5523 (1989).
- N. Maki et al., *J. Bacteriol.* **182**, 4337 (2000).
- F. Tetart et al., *Mol. Microbiol.* **6**, 621 (1992).
- H. H. McAdams, A. Arkin, *Proc. Natl. Acad. Sci. U.S.A.* **94**, 814 (1997).
- J. Paulsson, *Nature* **427**, 415 (2004).
- P. S. Swain, M. B. Elowitz, E. D. Siggia, *Proc. Natl. Acad. Sci. U.S.A.* **99**, 12795 (2002).
- M. Thattai, A. van Oudenaarden, *Proc. Natl. Acad. Sci. U.S.A.* **98**, 8614 (2001).
- We thank R. Kishony, B. Shraiman, U. Alon, R. Ranganathan, S. Altschuler, L. Wu, and K. Süel, together with members of the Elowitz laboratory, for thoughtful comments and discussions. This work was supported by grants from NIH (R01 GM079771 to M.B.E. and GM068763 to the Center for Modular Biology), the Searle Scholars Program, the Human Frontiers Science Program, and the Packard Foundation. G.M.S. is supported by California Institute of Technology Center for Biological Circuit Design and the University of Texas Southwestern's Endowed Scholars Program. J.G.O. acknowledges financial support from the Ministerio de Educación y Ciencia (Spain, project FIS2006-11452) and from the Generalitat de Catalunya.

#### Supporting Online Material

www.sciencemag.org/cgi/content/full/315/5819/1716/DC1  
Materials and Methods  
SOM Text  
Figs. S1 to S17  
Tables S1 to S4  
References

13 November 2006; accepted 26 February 2007  
10.1126/science.1137455

## Temporal Frequency of Subthreshold Oscillations Scales with Entorhinal Grid Cell Field Spacing

Lisa M. Giacomo,<sup>1\*</sup> Eric A. Zilli,<sup>1</sup> Erik Fransén,<sup>2</sup> Michael E. Hasselmo<sup>1\*</sup>

Grid cells in layer II of rat entorhinal cortex fire to spatial locations in a repeating hexagonal grid, with smaller spacing between grid fields for neurons in more dorsal anatomical locations. Data from in vitro whole-cell patch recordings showed differences in frequency of subthreshold membrane potential oscillations in entorhinal neurons that correspond to different positions along the dorsal-to-ventral axis, supporting a model of physiological mechanisms for grid cell responses.

The entorhinal cortex plays an important role in encoding of spatial information (1–3) and episodic memory (4). Many layer II neurons of rat entorhinal cortex are grid cells, firing when the rat is in an array of spatial locations forming a hexagonal grid within the environment

(5–7). The spacing of firing fields in the grid varies with anatomical position of the cell along the dorsal-ventral axis of entorhinal cortex, as measured by distance from the posthinal border (5). Neurons closer to the dorsal border of entorhinal cortex have shorter distances between firing fields. Computa-